Analysis of Communications Blackout for Pioneer Venus Entry Probes

William L. Grose,* R.A. Falanga,† and Kenneth Sutton†
NASA Langley Research Center, Hampton, Va.

Estimates of the maximum duration of communications blackout are presented for a proposed Pioneer Venus mission involving a multiprobe entry targeted to individual impact sites. Calculations of the inviscid flow about the probes have been made using both finite-rate chemistry and equilibrium chemistry computer codes. Equilibrium boundary-layer calculations, including ablation, are also presented both with and without the presence of alkali metal contaminants from the heat shield. Methods are described for estimating maximum electron density in the inviscid wake and the recirculation region at the base of the probes. The results presented provide a conservative basis for planning for storage and subsequent telemetry of data during the entry phase of the mission.

Nomenclature

e	= electron charge
f	= frequency
m	= electron mass
N_e	= electron number density
R	= radius
w	= probe mass
y	= normal distance from body
β	= probe ballistic coefficient
γ_E	= entry angle
δ	= shock standoff distance
ϵ_0	= electric permittivity of free space
θ_c	= cone half-angle

Subscripts

B	= base
cr	= critical
e	= boundary-layer edge
n	= nose
p	= plasma
s	= shoulder

Introduction

PREVIOUS experience has established the possibility of communications blackout during atmospheric entry of blunt-nosed vehicles.[1-4] Blackout occurs because of the interference from free electrons produced in the high-temperature plasma surrounding the vehicle. Thus, predicting blackout duration reduces essentially to determining electron number density in the plasma.

The problem of predicting electron number density is particularly difficult for the Pioneer Venus mission because of the antenna (*s*-band) location on the base of the probes. The signal propagation path from the antenna passes through three regions (see Fig. 1): 1) an inviscid region behind the bow shock wave, 2) a low-velocity recirculation region, and 3) a shear layer separating the other two regions. The complexity of the flowfield, with the likelihood of large departures from chemical equilibrium for portions of the entry trajectory, presents a formidable, if not impossible, task of rigorously determining flow properties and species concentrations in the probe's wake.

As an alternative, it is possible to approach the problem with suitable assumptions and approximations, so that a conservative estimate of maximum electron number density can be made. The present paper describes such an analysis for the proposed Pioneer Venus mission and defines an upper limit to the duration of communications blackout for the range of input conditions considered.

Mission Description

The Pioneer Venus mission has the scientific objective of investigating the Venusian atmosphere.[5] Two Pioneer spacecraft are scheduled for launch in 1978. The first spacecraft will function as an orbiter and study the upper atmosphere. The second spacecraft will function as a bus to transport one large and three identical small probes, which will enter the Venus atmosphere and be targeted to individual impact sites.

It is with the latter mission that this paper is concerned. The large and small probes carry instrumentation designed to measure atmospheric parameters down to the Venus surface. The bus will also carry instrumentation and collect data above 130 km before its destruction during entry. A sketch of the probes' geometry and their entry trajectories is shown in Fig. 2. Although a range of possible entry angles exists ($\gamma_E = -20°$ to $-45°$ for the large probe and $\gamma_E = -12°$ to $-90°$ for the small probes), only those trajectories with the shallowest entry are shown, a condition for which blackout duration of the telemetry communications (*s*-band, $f = 2.3$ Ghz) is maximum.

Inviscid Wake

Both a finite-rate chemical kinetics code and an equilibrium chemistry code were used to calculate the inviscid flow between the bow shock wave and the probe forebody. To insure a conservative estimate of N_e in the inviscid wake, the peak value of N_e calculated at the probe shoulder was used as the starting value for a frozen, isentropic expansion to ambient pressure.

Equilibrium solutions were obtained with an inverse flowfield program.[6] This program utilizes the thin shock-layer approximations of Maslen[7] and an approximate equation of state for an equilibrium mixture of 90% CO_2 – 10% N_2 composition by volume. The program has the option

Presented as Paper 75-182 at the AIAA 13th Aerospace Sciences Meeting, Pasadena, Calif., January 20-22, 1975; submitted February 10, 1975; revision received June 16, 1975.

Index category: Thermochemistry and Chemical Kinetics.

*Research Scientist, Analytical Studies Branch, Space Applications and Technology Division. Member AIAA.

†Research Scientist, Advanced Entry Analysis Branch, Space Systems Division. Member AIAA.

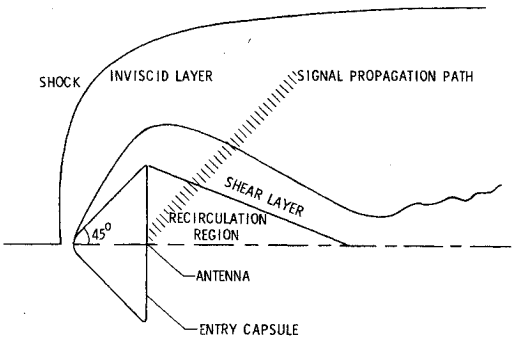

Fig. 1 Schematic of flowfield about entry probe.

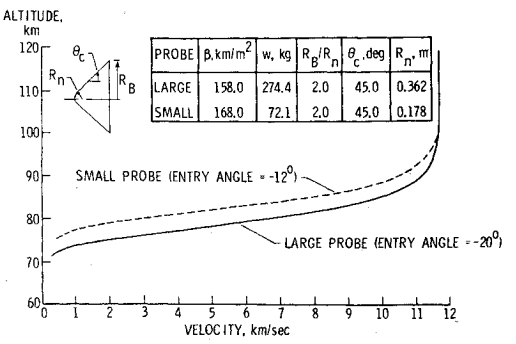

Fig. 2 Entry trajectory and probe geometry.

of computing either adiabatic (no heat loss) or nonadiabatic (radiation coupling) results. Both options were exercised, but only the adiabatic results, which yield higher electron number densities than the nonadiabatic results, are presented. This result is expected because the radiation cooling reduces the temperature in the shock layer near the wall and consequently produces less ionization than for the equivalent adiabatic case. A number of the equilibrium solutions were checked and are in agreement within 10-15% of so-called "benchmark" solutions obtained with the detailed, more exact method presented in Ref. 8. Calculations with the more exact method were obtained using both 90% CO_2-10% N_2 and 100% CO_2 atmosphere. No significant differences in N_e resulted because essentially all the electrons are produced from ionization of CO and C.

Severe departures from chemical equilibrium often occur during high-speed entry. To ascertain whether nonequilibrium effects might yield predictions of blackout duration different from the results of an equilibrium analysis, solutions were also obtained with the inverse, flowfield program described in Ref. 9. This program is also based upon the thin shock-layer approximations of Maslen.[7] The gas within the shock layer

Table 1 Kinetics mechanism (atmosphere of 97% CO_2-3% N_2 by volume)

Reaction	Forward rate constant[a]	Reverse rate constant[a]
1) $CO_2+M=C+O+M$	$1.2\times10^{11}T^{0.5}\exp(-34340/T)$	$2\times10^{6}T^{1.25}\exp(28400/T)$
2) $CO+M=C+O+M$	$4.48\times10^{19}T^{-1}\exp(-128900/T)$	$1+10^{18}T^{-1}$
3) $N_2+M=2N+M$	$2.46\times10^{19}T^{-1}\exp(-113200/T)$	$1.5\times10^{18}T^{-1}$
4) $NO+M=N+O+M$	$4.09\times10^{18}T^{-1}\exp(-75330/T)$	$3.5\times10^{18}T^{-1}$
5) $O_2+M=2O+M$	$9.05\times\times10^{18}T^{-1}\exp(-59370/T)$	$9.0\times10^{15}T^{-0.5}$
6) $CO+N=NO+C$	$2.86\times10^{11}T^{0.5}\exp(-53630/T)$	$2.6\times10^{10}T^{0.5}$
7) $2CO=CO_2+C$	$2.33\times10^{9}T^{0.5}\exp(-65710/T)$	$4.6+10^{12}T^{-0.25}$
8) $CO+O=O_2+C$	$2.73+10^{12}T^{0.5}\exp(-69540/T)$	$9.4\times10^{12}T^{0.25}$
9) $N_2+O=NO+N$	$7.35+10^{11}T^{0.5}\exp(-37940/T)$	$1.6\times10^{11}T^{-0.5}$
10) $NO+CO=CO_2+N$	$4.59+10^{8}T^{0.5}\exp(-12070/T)$	$9.9\times10^{12}T^{-0.25}$
11) $NO+\&=O_2+N$	$2.98\times10^{11}T^{0.5}\exp(-19460/T)$	$9.5+10^{9}T$
12) $CO_2+O=O_2+CO$	$2.54+10^{11}T^{0.5}\exp(-27690/T)$	$5.0\times10^{8}T\exp(-23900/T)$
13) $2O=O_2^{+}+e^{-}$	$5.42\times10^{10}T^{0.5}\exp(-80560/T)$	$7.2+10^{20}T^{-1.2}$
14) $C+O=CO^{+}+e^{-}$	$7.55+10^{10}T^{0.5}\exp(-33660/T)$	$1.08\times10^{21}T^{-1.2}$
15) $N+O=NO^{+}+e^{-}\exp(-32150/T)$	$2.43\times10^{10}T^{0.5}\exp(-32150/T)$	$4.0\times10^{20}T^{-1.2}$
16) $CO+NO^{+}=CO^{+}+NO$	$2.3\times10^{12}T^{0.5}\exp(-55190/T)$	1.5×10^{13}
17) $O_2+NO^{+}=O_2^{+}+No$	$2.2\times10^{12}T^{0.5}\exp(-32840/T)$	$4.0\times10^{11}T^{0.5}$
17) $O_2+O_2^{+}\,CO^{+}+O_2$	$2.2\times10^{12}T^{0.5}\exp(-22400/T)$	7.0×10^{13}
19) $O+NO^{+}=O_2^{+}+N$	$2.70\times10^{12}T^{0.5}\exp(-48730/T)$	$2.0+10^{12}T^{0.5}$

[a]Units of rate constant are cm^3 -$mole^{-1}$ -sec^{-1} or cm^6 -$mole^{-2}$ sec^{-1}. Rate constants were obtained: 1) from Ref. 10, 2) by collision theory, or 3) by deducing the forward value of the activation energy by net change in chemical bond energy and determining the remaining constants by analogy with known rates of a similar kind.

Table 2 Kinetics mechanism (atmosphere of 100% CO_2)

Reaction	Forward rate constant[a]	Reverse rate constant[a]
1) $CO_2+M=CO+O+M$	$1.2\times10^{11}T^{0.5}\exp(-34340/T)$	$2.0\times10^{6}T^{1.25}\exp(28300/T)$
2) $CO+M=C+O+M$	$4.48\times10^{19}T^{-1}\exp(-128900/T)$	$1.0+10^{18}T^{-1}$
3) $CO+C=C_2+O$	$1.14+10^{11}T^{0.5}\exp(-56600/T)$	$2.5\times10^{30}T^{-3.87}$
4) $C+O=CO^{+}+e-$	$7.55\times10^{10}T^{0.5}\exp(-33660/T)$	$1.08\times10^{21}T^{-1.2}$
5) $C+e-=C^{+}+2e-$	$4.0\times10^{13}T^{0.5}\exp(-130600/T)$	$1.84\times10^{21}T^{-0.836}$
6) $0+e-=O^{+}+2e-$	$4.0\times10^{13}T^{0.5}\exp(-158000/T)$	$1.13\times10^{22}T^{-1}$
7) $O_2+M=2O+M$	$9.05\times10^{18}T^{-1}\exp(-59370/T)$	$9.0\times10^{15}T^{-0.5}$
8) $2O=O_2^{+}+e-$	$5.42\times10^{10}T^{0.5}\exp(-80560/T)$	$7.2\times10^{20}T^{-1.2}$
9) $CO+e-=CO^{+}+2e-$	$4.0\times10^{13}T^{0.5}\exp(-162476/T)$	$1.6\times10^{21}T^{-0.955}$
10) $O_2+C^{+}=O_2^{+}+C$	$3.0\times10^{12}T^{0.5}\exp(-9511/T)$	$3.7\times10^{11}T^{0.7}$
11) $O+O_2^{+}=O^{+}+O_2$	$2.7\times10^{12}T^{0.5}\exp(-17746/T)$	$4.576\times10^{13}T^{0.256}$
12) $CO+C^{+}=CO^{+}+C$	$3.0\times10^{12}T^{0.5}\exp(-31900/T)$	$4.88\times10^{25}T^{-2.5}$
13) $CO+O^{+}=CO^{+}+O$	$2.7\times10^{12}T^{0.5}\exp(-4641/T)$	$3.06+10^{13}T^{0.2}$
14) $O+C^{+}=O^{+}+C$	$3.3\times10^{12}T^{0.5}\exp(-27260/T)$	9.43×10^{24}

[a]Units of rate constant are cm^3 -$mole^{-1}$ -sec^{-1} or cm^6 -$mole^{-2}$ sec^{-1}. Rate constants were obtained: 1) from Ref. 10, 2) by collision theory, or 3) by deducing the forward value of the activation energy by net change in chemical bond energy and determining the remaining constants by analogy with known rates of a similar kind.

undergores the processes of dissociation, recombination, vibrational excitation, electronic excitation, ionization, and charge transfer. Two kinetics mechanisms were assumed for the reported calculations. The mechanism used near emergence from blackout is given in Table 1 with an assumed composition of 97% CO_2-3% N_2 by volume. This mechanism is identical to that used in a blackout study for the Viking Mission[10] and is judged to be appropriate for the temperatures and velocities encountered in the shock layer at altitudes where emergence from blackout occurs. Including 3% N_2 by volume has the effect of predicting a conservative value of N_e. Most of the electrons are produced by reaction 15. At higher altitudes near beginning of blackout, temperatures and velocities in the shock layer are much greater and the mechanism shown in Table 2, assuming a composition of 100% CO_2, was judged appropriate. At these conditions the electron impact reactions (5-6) and the associative ionization of atoms reaction (4) become important and produce most of the electrons. Initial calculations were made using the full set in Table 2. After some experimentation, it was found that the program ran significantly faster and predicted higher electron number densities (less than 10% higher for all cases) by deleting charge formation reactions 8-9 and charge exchange reactions 10-14 than would result if they were retained. Subsequent calculations presented herein were made with the reduced set.

Recirculation Region

In the recirculation region, the flow residence time is assumed long relative to the time required to establish equilibrium. The flow in the recirculation region originates primarily from the boundary layer over the forebody of the probe and includes material ablated from the heat shield. The procedure for estimating N_e in this region consists of first calculating the boundary layer over the forebody using a computer code described in Ref. 11. This program assumes a nonsimilar, multicomponent boundary layer with mass injection, unequal diffusion coefficients, and arbitrary equilibrium chemistry. The cases to be presented assume steady-state ablation, and that transition to turbulent flow occurs at a momentum thickness Reynolds number of 250.

After calculating the boundary layer, an integrated average value of each elemental mass fraction at the probe shoulder is determined. It is this elemental composition that is assumed for the recirculation region. These values of elemental mass fraction, together with an appropriate pressure and temperature, and input into an equilibrium thermodynamics properties code[12,13] to calculate N_e. After surveying various pressure measurement studies, it is apparent that throughout the recirculation region the pressure is nearly constant.[3] An upper limit for the pressure in this region was chosen to be 0.015 of the stagnation pressure. A temperature appropriate to this region was estimated from an enthalpy parameter and Reynolds number dependence using the data of Refs. 14-22.

Past experience has demonstrated that most of the electrons in this region result from ionization of alkali metal contaminants from the heat shield. The proposed heat-shield material for the Pioneer Venus probes is a carbon-phenolic. Specifications restrict total alkali metal content to be less than 0.005 mass fraction of the ablator. To obtain conservative estimates of N_e, boundary-layer calculations were made assuming that all of the alkali metal contaminant was sodium and that it was present in amount equal to the specification value. For comparison, calculations were repeated with sodium of twice the specification value and with no sodium present.

Shear Layer

Estimates of N_e were not made for the shear layer because it seems plausible that electron density for this layer would not exceed that of both the inviscid wake and the recirculation region.[3] This assumption is based upon the reasoning that, should more ionization exist in the shear layer than exists in the inviscid wake, the recirculation region would exhibit even greater ionization because the temperatures are as high or higher and the particle residence times are longer than for the shear layer.

Criterion for Blackout

A sudden rise in attenuation of a communications signal by a plasma occurs when the plasma frequency

$$f_P = (e/2\pi)\ (N_e/m\epsilon_0)^{1/2} \tag{1}$$

equals the communications signal frequency.[3] For the s-band frequency of 2.3 GHz for the Pioneer Venus probes the critical value of N_e for which this occurs is 6.56×10^{10} cm^{-3}. The level of attenuation depends upon the signal path length through the plasma as well as N_e. Because of the lack of knowledge of the geometry of the wake flow and of the N_e distribution, it is not practical to make attenuation calculations.

Depending upon the characteristics of the communications system, a certain amount of attenuation can be tolerated. However, for the purposes of determining an upper bound to communications blackout duration, blackout is said to occur when the estimated N_e of the inviscid wake or the recirculation region exceeds this critical value.

Results

Some typical profiles of N_e across the inviscid shock layer at the shoulder of the probe are shown for altitudes of 89.09 km and 120.23 km in Fig. 3. It can be observed that, although the peak value of N_e is not too different for the equilibrium and nonequilibrium cases, the thickness of the high N_e layer is much less, particularly for the higher altitude. The im-

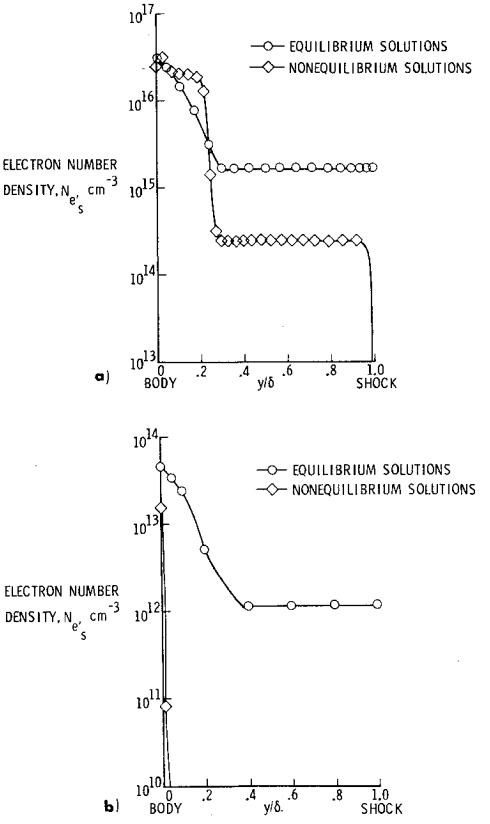

Fig. 3 Electron number density profiles across inviscid shock layer at shoulder of large probe. a) Altitude of 89.09 km. b) Altitude of 120.23 km.

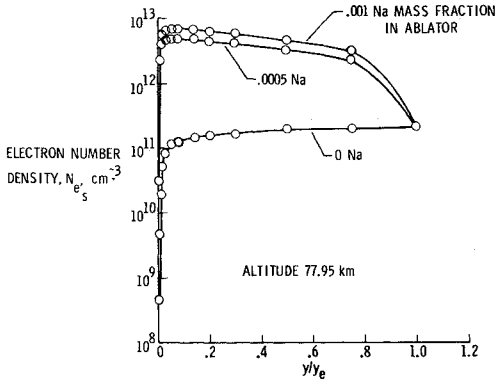

Fig. 4 Electron number density profiles across boundary layer at shoulder of large probe.

portance of this observation will become apparent when estimates of blackout duration are presented.

The rather sudden drop in N_e for the nonequilibrium case shown in Fig. 3b results from the low collision rate at this altitude. The nonequilibrium region occupies much of the total shock layer, in contrast to the case shown in Fig. 3a where the nonequilibrium effects are confined to a region close to the shock front. Particle residence times are much lower for the outermost streamlines than for the body streamline.

A typical profile of N_e across the boundary layer at the shoulder of the large probe is shown in Fig. 4. Comparisons of N_e are shown for 1) no sodium in the heat shield, 2) sodium mass fraction in heat shield of 0.0005 (specification level), and 3) sodium mass fraction in heat shield of 0.001. The significant increase in N_e due to the presence of small amounts of contaminant is readily apparent. For all three cases, the level of N_e is fairly constant over much of the boundary layer.

Calculations of peak N_e as a function of time (zero time occurs at 248.5 km) and altitude for both the inviscid wake and the recirculation region are shown in Fig. 5. For the large probe ($\gamma_E = -20°$) results shown in Fig. 5a, the adiabatic, equilibrium calculations for the inviscid wake indicate a blackout duration of approximately 13 sec. The nonequilibrium calculations predict essentially the same result. However, recalling Fig. 3, the thickness of the high N_e layer at the probe shoulder is significantly less for the nonequilibrium case at the higher altitude and would result in less attenuation of a signal than for the equilibrium case. Conseqently, nonequilibrium effects indicate that onset of blackout would occur somewhat later than predicted here by using the peak value of N_e for the analysis. At these altitudes, the heating rate to the body is so low that no significant ablation occurs and therefore very little ionization exists in the recirculation region.

At lower altitudes, nonequilibrium effects are no longer present and the rapid decrease in N_e with altitude clearly identifies termination of blackout. Peak N_e values for the recirculation region (N_A mass fraction in ablator of 0.0005) are considerably higher than for the inviscid wake. However, because of the rapid decrease in N_e with altitude, these results indicate a delay in termination of approximately 1 sec compared to the inviscid results. For comparison purposes, the critical value of N_e for x-band frequency of 9 GHz is shown on the figure.

The results for the small probe ($\gamma_E = -12°$) shown in Fig. 5b are qualitatively similar to the results shown for the large probe. Blackout duration is approximately 28 sec based upon the adiabatic, equilibrium calculations for the inviscid wake. Values of N_e for the recirculation region predict termination of blackout approximately 2 sec later.

Because the three small probes will be targeted to different impact sites, adiabatic, equilibrium calculations for the inviscid wake were also conducted for $\gamma_E = -20°$ and $\gamma_E = -70°$. The results shown in Figs. 5c and 5d, respectively, predict blackout durations of approximately 13 sec and 5 sec.

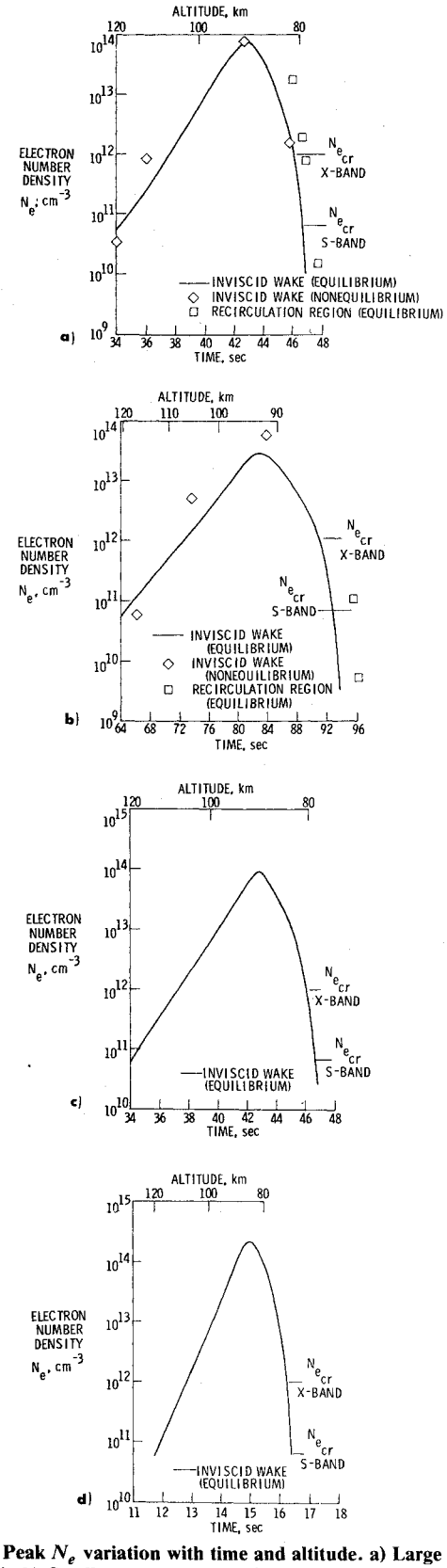

Fig. 5 Peak N_e variation with time and altitude. a) Large probe ($\gamma_E = -20°$). b) Small probe ($\gamma_E = -12°$). c) Small probe ($\gamma_E = -20°$). d) Small probe ($\gamma_E = -70°$).

A summary of the adiabatic, equilibrium results for the inviscid wake is shown in Fig. 6. If one assumes as a rule-of-thumb (suggested by S. Somer, Project Pioneer, NASA Ames

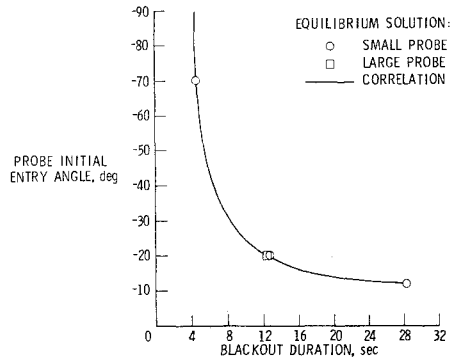

Fig. 6 Blackout duration as a function of entry angle.

Research Center) that blackout onset occurs at the same altitude for all γ_E and terminates at the same velocity for all γ_E, then the solid curve results from using the large probe ($\gamma_E = -20°$) calculations and applying the rule to the trajectories appropriate for other entry angles. Interestingly, the agreement with the small probe results ($\gamma_E = -12°$ and $-70°$) is excellent, These results imply that, for entry angles shallower than about $-20°$, blackout duration increases rapidly as a function of entry angle. However, the reader must be cautioned that the calculated points are only for the inviscid wake and are based upon equilibrium, adiabatic results. As pointed out earlier, realistic assessment of nonequilibrium effects indicates onset of blackout occurring later than shown in the predictions. Furthermore, consideration of ablation products in the recirculation region could shift the point of emergence from blackout.

Conclusions

Estimates of the duration of communications blackout for Pioneer Venus entry probes have been presented. Maximum duration of blackout is approximately 13 sec for the large probe and 28 sec for the small probe. For entry angles shallower than approximately $-20°$, blackout duration increases rapidly as a function of entry angle.

Because of various uncertainties and the complexity of the flowfield, it must be emphasized that the results are intended as a conservative upper bound to serve as a basis for planning for storage and subsequent telemetry of data during entry. Actual blackout, if it indeed occurs, may be less than indicated by the results presented here.

References

[1] Huber, P.W. and Sims, T.E., "The Entry-Communications Problem," *Astronautics & Aeronautics*, Vol. 2 Oct. 1964, pp. 30-40.

[2] Evans, J.S., and Huber, P.W., "Calculated Radio Attenuation due to Plasma Sheath on Hypersonic Blunt-Nosed Cone," NASA, TN D-2043, Dec. 1963.

[3] Huber, P.W., "Deduction of Reentry Plasma Properties about Manner Orbital Spacecraft from Radio Signal Attenuation Data," NASA TN D-4118, 1962.

[4] Huber, P.W., Evans, J.S., and Schexnayder, C.J., Jr., "Comparison of Theoretical and Flight-Measured Ionization in a Blunt Body Re-Entry Flowfield," *AIAA Journal*, Vol. 9, June 1971, pp. 1154-1162.

[5] Dyer, J.W., Nunamaker, R.R., Cowley, J.R., and Jackson, R.W., "Pioneer Venus Mission Plan for Atmospheric Probes and an Orbiter," *Journal of Spacecraft and Rockets*, Vol. 11, Oct. 1974, pp. 710-715.

[6] Falanga, R.A. and Olstad, W.B., "Approximate Inviscid Radiating Flowfield Analysis for Sphere-Cone Venusian Entry Vehicles," AIAA Paper 74-758, *1974 AIAA/ASME Thermophysics and Heat-Transfer Conference*, Boston, Mass., July 1974.

[7] Maslen, S.H., "Inviscid Hypersonic Flow Past Smooth Symmetric Bodies," *AIAA Journal*, Vol. 2, June 1964, pp. 1055-1061.

[8] Sutton, K., "Coupled Nongray Radiating Flow about Ablating Planetary Entry Bodies," *AIAA Journal*, Vol. 12, Aug. 1974, pp. 1099-1105.

[9] Grose, W.L., "Thin-Shock-Layer Solution for Nonequilibrium, Inviscid Hypersonic Flows in Earth, Martian, and Venusian Atmospheres," NASA TN D-6529, Dec. 1971.

[10] Evans, J.S.,Shexnayder, C.J., Jr., and Grose, W.L., "Effects of Nonequilibrium Ablation Chemistry on Viking Radio Blackout," *Journal of Spacecraft and Rockets*, Vol. 11, Feb. 1974, pp. 84-88.

[11] Anderson, L.W. and Morse, H.L., "User's Manual—Volume I: Boundary-Layer Integral Matrix Procedure (BLIMP)," Tech. Rept. AFWL-TR-69-114, Vol. I (Suppl.), Air For Weapons Lab., Kirtland AFB, N.M., 1971.

[12] Nicolet, W.E., "Advanced Methods for Calculating Radiation Transport in Ablation-Product Contaminated Boundary Layers," Contractor Rept., NASA CR-1656, 1970.

[13] Nicolet, W.E., "User's Manual for the Generalized Radiation Transfer Code (RAD/EQUIL)," Aerotherm Rept. No. UM-69-9, Aerotherm Corp., Mountain View, Calif. (available as NASA CR-116353, 1969.)

[14] Huber, P.W. and Hunt, J.L., "Reynolds Number Dependence of Apollo Near Wake Temperature," *AIAA Journal*, Vol. 6, Jan. 1968, pp. 184-185.

[15] Weiss, R.F. and Weinbaum, S., "Hypersonic Boundary-Layer Separation and the Base Flow Problem," Research Rept. 221, July 1965, Avco-Everett Research Labs., Everett, Mass.

[16] Todisco, A. and Pallone, A.J., "Near Wake Flowfield Measurements," *AIAA Journal*, Vol. 3, Nov. 1965, pp. 2075-2080.

[17] Zakkay, V. and Cresci, R.J., "Experimental Investigation of the Near Wake of a Slender Cone at $M_\infty = 8$ and 12, *AIAA Journal*, Vol. 4, Jan. 1966, pp. 41-46.

[18] Martellucci, A., Trucco, H., and Agone, A., "Measurements of the Turbulent Near Wake of a Cone at Mach 6," *AIAA Journal*, Vol. 4, March 1966, pp. 385-391.

[19] Muntz, E.P. and Softley, E.J., "Study of Laminar Near Wakes," *AIAA Journal*, Vol. 4, June 1966, pp. 961-968.

[20] Todisco, A., and Pallone, A., "Measurements in Laminar and Turbulent Near Wakes," AIAA Paper 67-30, New York, 1967.

[21] Reeves, B.L. and Lees, L., "Theory of Laminar Near Wake of Blunt Bodies in Hypersonic Flow," *AIAA Journal*, Vol. 3, Nov. 1965, pp. 2061-2074.

[22] Beckwith, I.E., Bushnell, D.M., and Huffman, J.K., "Investigation of Water Injection on Models of Gemini Vehicle and Resulting Predictions for GT-3 Reentry Communications Experiment," (U), NASA TM X-1200, March 1966.